A fluidization transition of the cell envelope sets up a universal volume expansion pacemaker

Avik Mukherjee, Yanqing Huang, Seungeun Oh, Carlos Sanchez, Yu-Fang Chang, Xili Liu, Gary Andrew Bradshaw, Nina Catherine Benites, Johan Paulsson, Marc W. Kirschner, Yongjin Sung, Jens Elgeti, Markus Basan[#]

[#] Correspondence: markus@hms.harvard.edu

The bacterial cell wall is a complex and resource-intensive biochemical structure that must expand in concert with biomass growth to prevent lysis or molecular crowding. Elegant experiments have shown that cell volume growth continues largely unperturbed in the face of periodic osmotic shocks, raising the question how the pace of cell wall expansion is regulated in *E. coli*. We discovered a proportional relationship of turgor pressure with growth rate. Remarkably, despite this increase in turgor, cellular biomass density was constant across a wide range of growth rates. In contrast, perturbing turgor away from this scaling directly affected density. To understand these confusing observations, we formulated a mathematical model, in which endopeptidase-mediated cell wall fluidization enables turgor pressure to set the pace of cellular volume expansion. This model not only explains our observations but makes a set of non-trivial predictions that we tested experimentally. As predicted, we found that modulating the effective viscosity of the cell wall was sufficient to control cellular biomass density. We also validated a surprising inverse relationship between cell width and biomass density. A remaining puzzle was what mediates the increase in turgor pressure with growth rate. The picture that emerges is that changes in turgor pressure across growth rates are mediated by changes in the concentration of counterions, balancing the net charge of ribosomal RNA. Profoundly, the coupling between rRNA and pressure simultaneously coordinates cell volume expansion across growth rates and exerts homeostatic feedback control on cytoplasmic density, explaining the rapid adjustment of cell volume to total biomass after perturbations. Physical forces generated via this universal mechanism may drive the expansion of fast-growing, ribosome-dense cells in their local environment, ranging from microbes to aggressive cancers.

Cells must coordinate biomass production in the cytoplasm and biosynthesis and expansion of the cell envelope (Fig. 1A). Turgor pressure is the osmotic pressure exerted by the cytoplasm on the cell wall. To better understand the physiological role of turgor pressure in this process, we wanted to quantify the growth rate dependence of turgor pressure. Measuring turgor pressure is challenging because pressure exerted by the cytoplasm is directly balanced by the cell envelope (*1*) and therefore not easily accessible. One method to assess the magnitude of turgor pressure, pioneered by the lab of KC Huang, involves applying osmotic shocks to bacteria to induce plasmolysis (*2*). When bacteria are in plasmolysis, the cytoplasm is compressed and detached from the cell wall at the bacterial poles (Fig. 1B). During plasmolysis, cytoplasmic osmotic pressure is directly balanced by external osmolarity. By measuring the fold-change in cytoplasmic volume as a function of the applied osmolarity, it is then possible to calculate turgor pressure of the cell before the osmotic shock (Fig. S1). When we determined turgor pressure of *E. coli* in different growth conditions, we discovered a striking linear increase of turgor pressure with growth rate, ranging over more than an order of magnitude (Fig. 1C & Fig. S1).

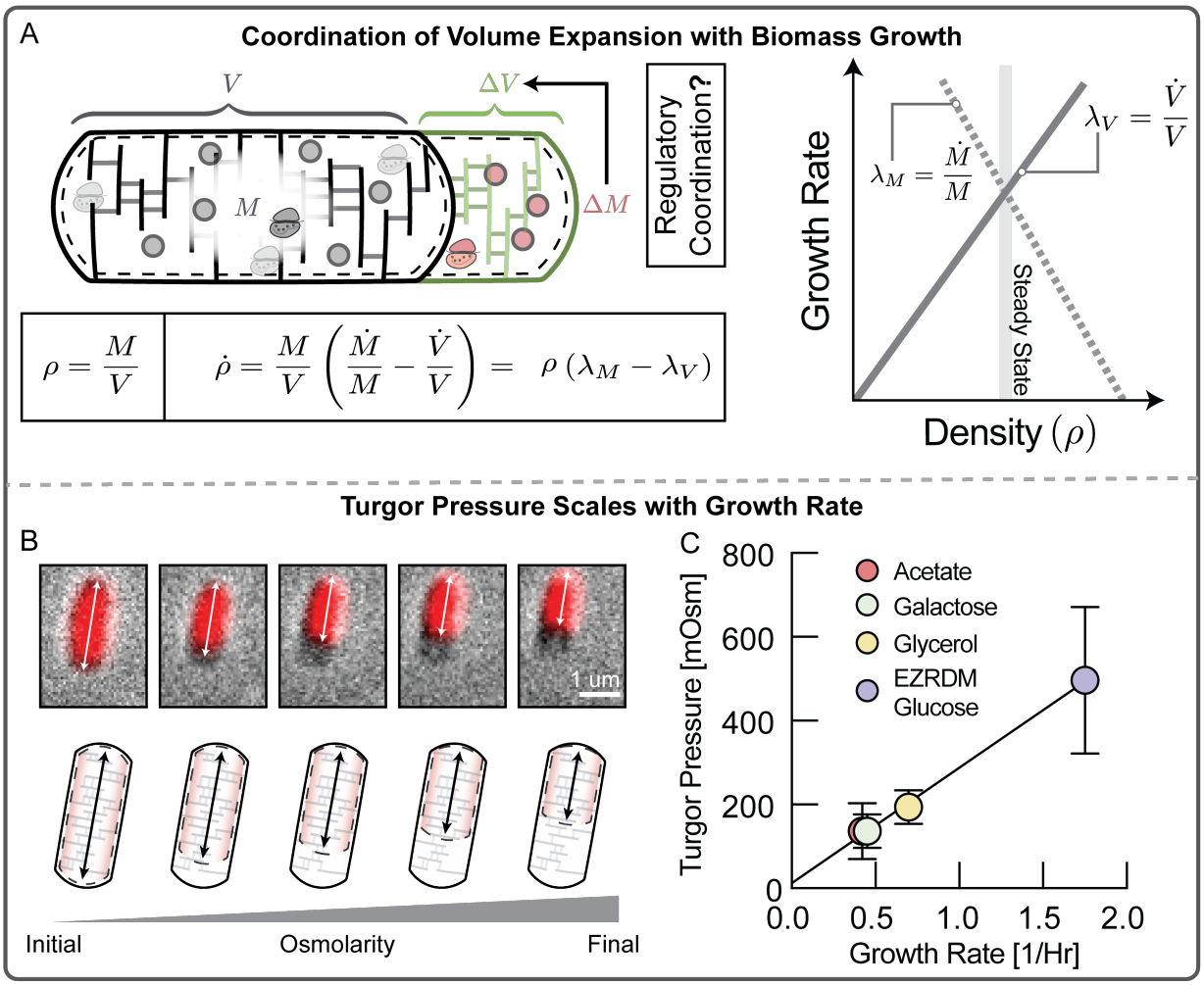

Figure 1: Turgor pressure increases with growth rate. A, *To achieve homeostasis of biomass density, addition of biomass ΔM to the cytoplasm must be coordinated with a corresponding increase in cell volume ΔV. The increase in cell volume comes from the expansion of the bacterial cell wall, a chemically complex, load-bearing structure, whereas biomass production occurs in*

the cytoplasm largely via ribosomal protein synthesis. It is currently unknown how these two fundamental cellular processes are kept in concert and coordinated across a wide range of growth rates. ***B,*** *Osmotic shocks put cells into plasmolysis, a state where the cytoplasm is retracted from the cell wall and osmotic pressure of the cytoplasm is balanced by externally applied osmolarity. Cytoplasmic volume before and after the shift can be measured using a fluorescent cytoplasmic marker.* ***C,*** *Turgor pressure in different growth conditions plotted against corresponding growth rates in these conditions. Fits to the Boyle-van't Hoff equation underlying these data, originating from osmotic shocks of different magnitude are presented in Fig. S1. Individual data points in Fig. S1 represent biological replicates and each of these data point results from averaging 13 randomly selected cells undergoing this osmotic shock. Error bars represent uncertainty of the fit of the slope to the data in Fig. S1.*

But what is the physiological role of this this surprising coordination of turgor pressure with growth rate? Turgor pressure results in tension in the cell wall and it has been established that mechanical forces can influence cell wall elongation in *E. coli* (*3*). Therefore, we hypothesized that increasing turgor pressure with growth rate could coordinate expansion of the cell envelope with growth rate (Fig. 2A). Faster growth requires faster expansion of the cell envelope, and it is presently not clear how bacteria achieve this coordination. The increase in turgor pressure observed in Fig. 1 could mediate faster cell wall expansion, thereby keeping the density of biomass constant across growth rates (Fig. 2A).

To test this hypothesis, we sought to measure the effect of changing turgor pressure on biomass density. If turgor pressure were indeed required for driving cell volume expansion across growth rates, perturbing turgor pressure should directly affect biomass density. We used quantitative phase microscopy to simultaneously measure cell mass and volume and (see Fig. S2-4 & Materials and Methods) and found that biomass density was remarkably constant across a large range of growth rates on different substrates (Fig. 2B & Fig. S5), consistent with previous observations (*4*, *5*). In contrast, hyperosmotic growth conditions that have been shown to reduce turgor pressure(*6*), resulted in higher biomass density and slower steady-state growth rate (Fig. 2C). To control turgor pressure more directly, we genetically titrated glutamate, which is the most abundant intracellular metabolite with concentrations of about 100mM (*7*). We used a strain developed by the Hwa lab, in which glutamate producing enzymes were placed under an inducible promoter (*8*, *9*). We confirmed this construct's ability to titrate intracellular glutamate by measuring intracellular glutamate for different induction levels (Fig. S6). Indeed, by titrating intracellular glutamate, it was possible to control cellular biomass density (Fig. 2D). The effect was comparable to the effect of higher medium osmolarities (Fig. 2C), consistent with the interpretation that both perturbations affect turgor pressure.

To better understand the control of cell volume growth via turgor pressure, we formulated a simple mathematical model summarized in Box 1 and Supplementary Note 1. Our goal was to find a minimal, coarse-grained description of the rheological properties of the cell wall, incorporating the effect of mechanics, including the key features of both experimental observations (*5*, *10*) and previous models(*3*, *11*, *12*). There is ample experimental evidence that cell wall elongation of *E. coli* can be influenced by mechanical stress (*3*, *12*). For instance, it has been shown that spatially confining *E. coli* in wells, deformed the bacterial envelope and when the bacteria were removed from the wells, cells maintained this new geometry for some time, before slowly relaxing back to the straight rod shape(*3*). Similarly, mechanical forces from fluid flow in microfluidic devices can

plastically deform growing *E. coli* cells and make them grow in a curved, rather than straight rod shape (*12*). Mechanical coupling with growth could emerge from cell wall mechano-endopeptidases that remodel the cell wall in stress-dependent way (*3*). It has been shown theoretically that an elastic material with stress-dependent remodeling behaves like a viscoelastic Maxwell material and can be modeled as a fluid on long timescales (*13*). Moreover, even constant activity of cell wall endopeptidases can result in cell wall fluidization, as illustrated in Box 1 (top), and similar to previous models of dislocation-mediated growth of the bacterial cell wall (*14*).

We therefore model the cell wall as a viscoelastic Maxwell fluid that behaves as an elastic on short timescales and as a viscous fluid on long timescales along its axis of elongation(*15*). As illustrated in Box 1 (bottom), this viscoelastic model naturally results in a volume expansion rate $\dot{V}/V$ that is directly proportional to turgor pressure. Thus, if turgor pressure is proportional to growth rate, as we observe experimentally (Fig. 1), this is precisely the dependence required as the pacemaker of cell volume growth to keep dry mass density constant across growth rates (see Fig. 2A & Supplementary Note 1, Eq. [S5]).

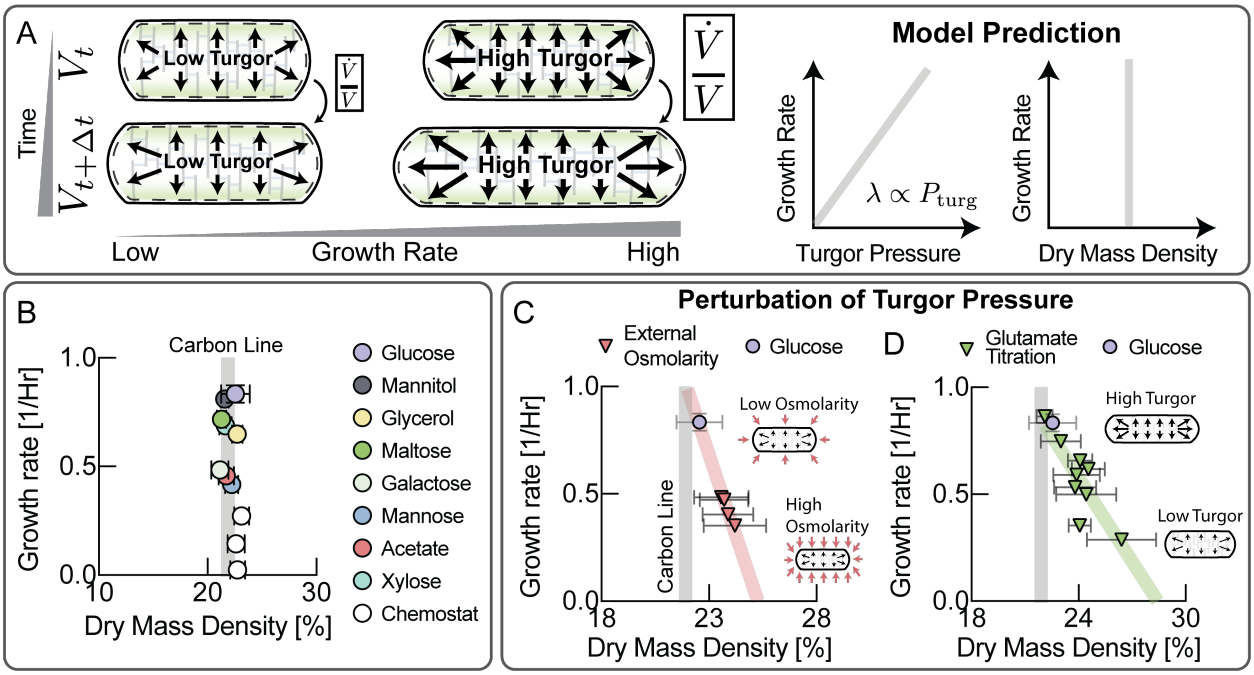

Figure 2: Turgor pressure coordinates cell envelope expansion with biomass growth. A, *We hypothesized that the physiological role of the observed increase in turgor pressure with growth rate in Fig. 1 is to coordinate growth rate of cell volume with growth rate of biomass. A linear increase of turgor pressure with growth rate ensures that biomass density remains constant across growth rates.* ***B,*** *Quantitative phase microscopy measurements show that biomass density is indeed remarkably constant across a wide range of growth conditions. Data for rich defined media is shown in Fig. S5. Growth rates are averages of biological replicates. Error bars in growth rate are the standard deviation from these biological replicates. Plotted dry mass density values result from averaging mean dry mass densities for the measured cell population from different biological replicates. Error bars in dry mass density were determined by propagating the standard deviations of the single cell distributions of the different measurements (Acetate: 3 measurements from n=3*

biological replicates; Glucose: 5 measurements from n=4 biological replicates; Glycerol: 6 measurements from n=6 biological replicates; Galactose: 1 measurement from 1 biological replicate; Maltose: 9 measurement from 7 biological replicates; Mannitol: 5 measurements from n=4 biological replicates; Xylose: 3 measurements from n=3 biological replicates; Chemostat conditions: 2 measurements from 2 biological replicates for each data point). Carbon line represents the average dry mass density of different carbon conditions shown in this panel except chemostat experiments ***C,*** *Cells become dense and growth rates slow down when grown in hyperosmotic media that reduce turgor pressure(6). Individual biological replicates plotted. Error bars are the standard deviation of the single cell distribution of the biological replicate.* ***D,*** *Reducing turgor pressure by titration of intracellular glutamate results in higher biomass density and slower growth, similar to the effect of external osmolarity. Individual experiments for different induction levels and biological replicates were binned by their measured growth rate (increments of 0.05/Hr). Error bars were determined by propagating the standard deviation of the single cell distributions from the individual experiments in each bin.*

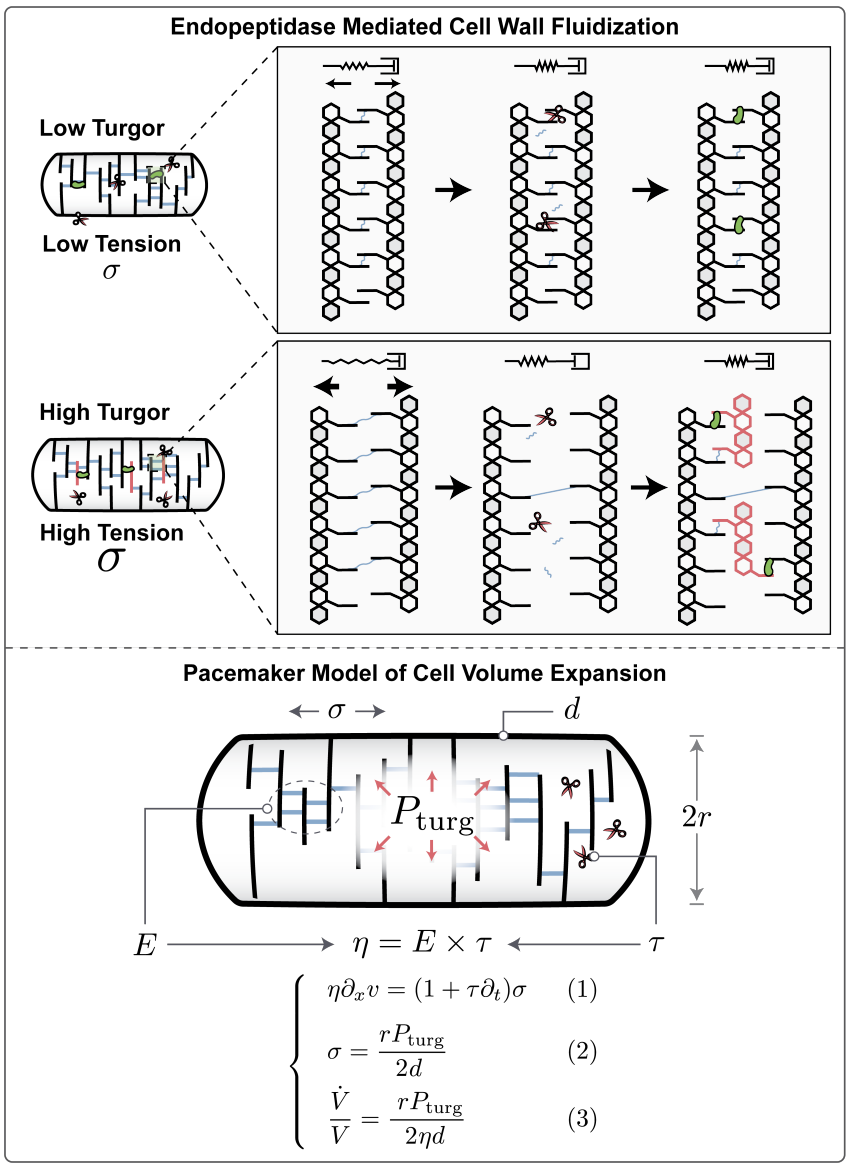

Box 1: Endopeptidase mediated cell wall fluidization (top). *Cell wall endopeptidases (scissors) cleave longitudinal peptide bonds that limit cell wall expansion. This leads to expansion of the peptidoglycan network dependent on cell wall stress generated by turgor pressure (middle panel), enabling insertion of new strands (red, right panel). Endopeptidases thus lead to stress-dependent expansion of cell wall material, resulting in stress relaxation. This constitutes a fluid-like rheology. Therefore, we model the cell wall as a Maxwell viscoelastic material, illustrated by the spring and damper in series. On short timescales such a material behaves like an elastic, whereas on long timescales it exhibits stress-dependent viscous flow that results in cell wall expansion.* ***Pacemaker model of cell volume expansion (bottom).*** *The cell wall is modeled as a Maxwell viscoelastic material with a constitutive equation, given by Eq. [1]. Turgor pressure P_{turg} from the cytoplasm acts on the cross-section of the cell, generating a tension σ in the cell wall that is given by Eq. [2]. Combining Eq. [1] with Eq. [2] and integrating over the length of the cell, the model predicts a simple expression for volume growth rate, given by Eq. [3]. Model parameters are summarized in Fig. S7. Model details and derivation of model predictions are presented in Supplementary Note 1.*

Beyond recapitulating our experimental findings, this model makes a set of non-trivial predictions how cell wall properties and cell shape affect biomass density that we tested experimentally: According to the model, cell wall rheology on long times is determined by an effective viscosity, given by $\eta = E\,\tau$, where E is the elastic modulus of the elastic network of the cell wall and τ is the viscoelastic relaxation time, which reflects cell wall remodeling by endopeptidases. Therefore, one way to affect cell wall viscosity is changing the rate of remodeling of the cell wall due to endopeptidase limitation (*13*). As illustrated in Fig. 3A, downregulating the abundance of cell wall endopeptidases should result in higher cell wall viscosity, slowing down volume growth rate, according to Box1, Eq. [3]. Higher viscosity from lower hydrolase abundance must thus be compensated by a combination of slower growth rates, greater cell widths or higher dry mass densities, as reflected in the model prediction (Fig. 3B & Supplementary Note 1, Eq. [S13]).

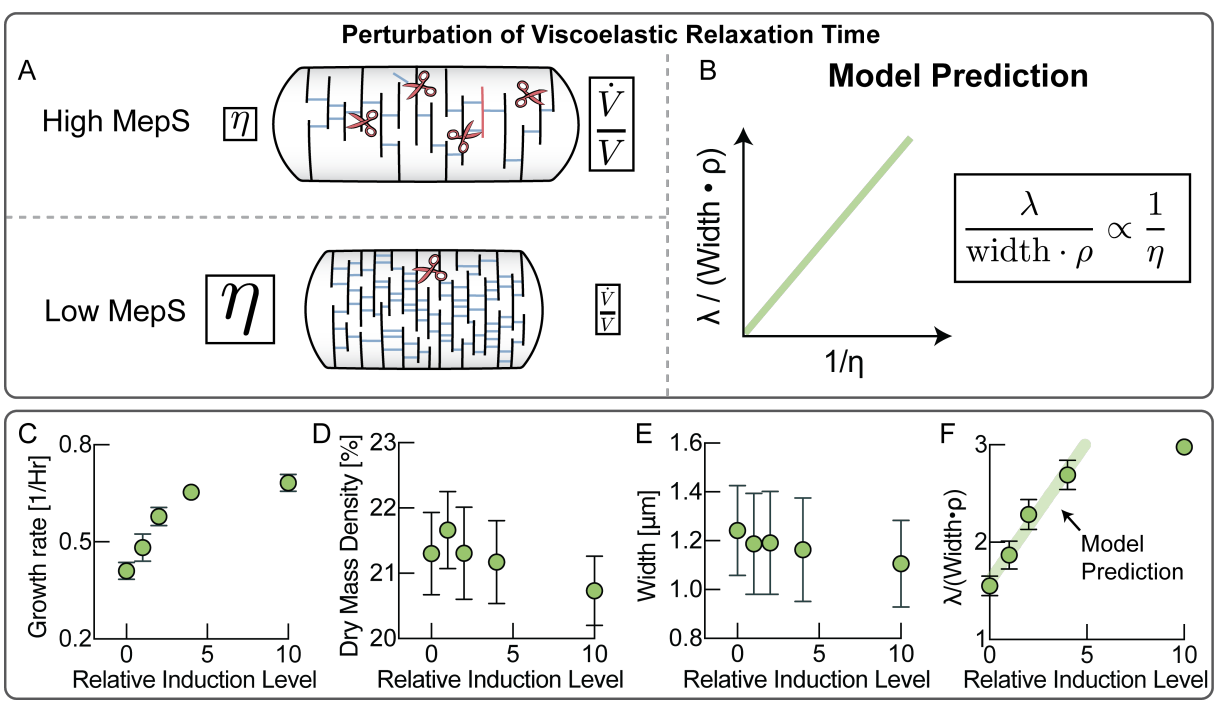

Figure 3: Cell wall viscosity can be controlled by endopeptidase titration. A, *Titration of the abundance of cell wall endopeptidases affects the effective viscosity of the cell wall, resulting in a slower volume growth rate with lower expression levels.* ***B,*** *The model predicts that increasing cell wall viscosity must be compensated by a combination of growth rate, biomass density and cell width (see Supplementary Note 1, Eq. [S13]).* ***C,*** *Growth rate as a function of induction levels of endopeptidase expression (number of biological replicates per induction level: 0: 6 replicates; 1: 6 replicates; 2: 5 replicates; 4: 4 replicates; 10: 6 replicates. Error bars represent standard deviation).* ***D,*** *Biomass density as a function of induction levels of endopeptidase expression. Biological replicates identical to panel C. Error bars represent standard deviation, propagated form biological replicates* ***E,*** *Cell width as a function of induction levels of endopeptidase expression. Biological replicates identical to panel C. Error bars represent standard deviation, propagated form biological replicates* ***F,*** *Comparison of experimental data to model prediction. A non-zero y-intercept can emerge from the activity of other cell wall endopeptidases. Error bars are standard deviations of the values calculated from the mean of individual biological replicates. Biological replicates identical to panel C.*

Experimentally, controlling endopeptidase activity is challenging because there are many redundant cell wall hydrolases in *E. coli*. Fortunately, a recent work identified three cell wall hydrolases that are together essential for growth of *E coli* (*16*). We therefore knocked out two of these hydrolases (MepM, MepH) and replaced the chromosomal promoter of the third (MepS) by a linearly inducible induction system (*17*). Indeed, at low induction levels, growth rate depended strongly on MepS induction levels (Fig. 3C). As expected from the model, low hydrolase expression also resulted in a combination of denser cells (Fig. 3D) and larger cell widths (Fig. 3E). Plotted in combination, these data show agreement with the model prediction over the linear induction range (Fig. 3F).

A different way to alter the effective viscosity of the cell wall according to the model is to experimentally perturb the elasticity of the cell wall. Ampicillin is a beta-lactam antibiotic that blocks cell wall crosslinking and insertion of new material into the cell wall (*18*). Ampicillin thereby results in a decreased crosslinking density and a softer, more elastic cell wall (smaller elastic modulus E and effective viscosity η, see Fig. 4A). According to Box1, Eq. [3], this decrease in effective viscosity should thus result in a faster volume expansion rate (Fig. 4B & Supplementary Note 1, Eq. [S10]). Indeed, we found that increasing sub-lethal concentrations of ampicillin continuously decreased cellular dry mass density during steady-state growth (Fig. 4C), while growth rates were approximately constant.

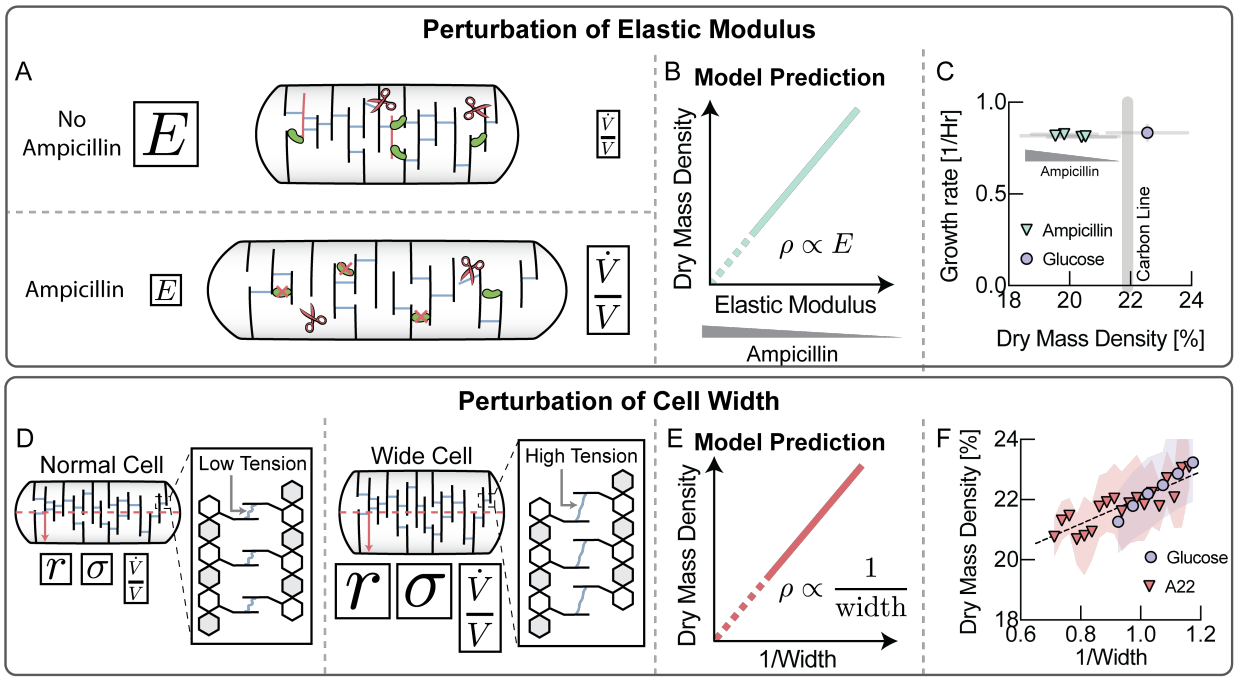

Figure 4: Cell wall elasticity and cell width alter biomass density. A, *Ampicillin affects the crosslinking density of the peptidoglycan network and thereby its elastic modulus. The elastic modulus of the cell wall is proportional to its effective viscosity and therefore controls volume growth rate.* ***B,*** *The model predicts a direct proportionality between biomass density and the elastic modulus of the cell (see Supplementary Note 1, Eq. [S10]).* ***C,*** *Sublethal doses of ampicillin resulted in decreasing biomass densities, while growth rate was unaffected. Error bars represent standard deviation of DMD from the distribution cells measured in each experiment.* ***D,*** *A larger cell width results in higher cell wall tension and therefore a higher volume expansion rate.* ***E,*** *The model predicts that faster volume expansion rate due to higher cell width must be compensated by a drop in biomass density (see Supplementary Note 1, Eq. [S8]).* ***F,*** *Average biomass density of individual cells binned by their inverse cell width drops with increasing width. The effect is amplified by inhibiting MreB using A22 and also holds when pooling data across different carbon sources (see Fig. S8). Glucose bin increment: 0.05μm^{-1}. A22 bin increment: 0.025μm^{-1}. Shaded areas represent the standard deviation of the distribution of cells in each bin.*

The model also makes a surprising prediction regarding the effect of cell width on biomass density (Fig. 4D). According to Box1, Eq. [3], volume growth rate of the cell should be directly affected by cell width because turgor pressure creates tension in the cell wall by acting on the cellular cross section. This force scales quadratically with the width and this force is distributed along the circumference, which scales linearly with cell width, to generate cell wall tension. Therefore, cell wall tension and the expansion rate of the cell should increase linearly with cell width. Because growth rate is limited by biomass production, higher tension from increasing widths must be compensated by lower turgor pressure. Assuming that turgor pressure is proportional to biomass density (an assumption that will be justified below), the model predicts a simple inverse proportionality between biomass density and width (Fig. 4E & Supplementary Note 1, Eq. [S8]). Indeed, in qualitative agreement with the model, binning cells in a growing population on glucose minimal medium according to their width, we confirmed this surprising dependence of biomass

density on cell width (Fig. 4F, blue circles). This effect was also reflected in data across different growth conditions (Fig. S8). When we inhibited MreB, a protein known to be involved in regulation of cell width in *E. coli* (*19*, *20*), we found a similar, if amplified relationship between biomass density and cell width (Fig. 4F, red triangles). These data demonstrate that cell width indeed exerts a surprising effect on cellular biomass density, as predicted by the model (Box 1).

The only remaining model parameter, affecting volume expansion rate according to Box1, Eq. [3] that we had not yet perturbed, was the thickness of the cell wall. The cell wall in *E. coli* is a monolayer and thus cell wall thickness cannot easily be modified experimentally. However, gram positive bacteria like *B. subtilis* have similar growth rates and a chemically similar, but much thicker multi-layered cell wall. Interestingly, estimates suggest that *B. subtilis* also has a much larger turgor pressure than *E. coli* (Fig. S9), consistent with the model expectation from Box1, Eq. [3].

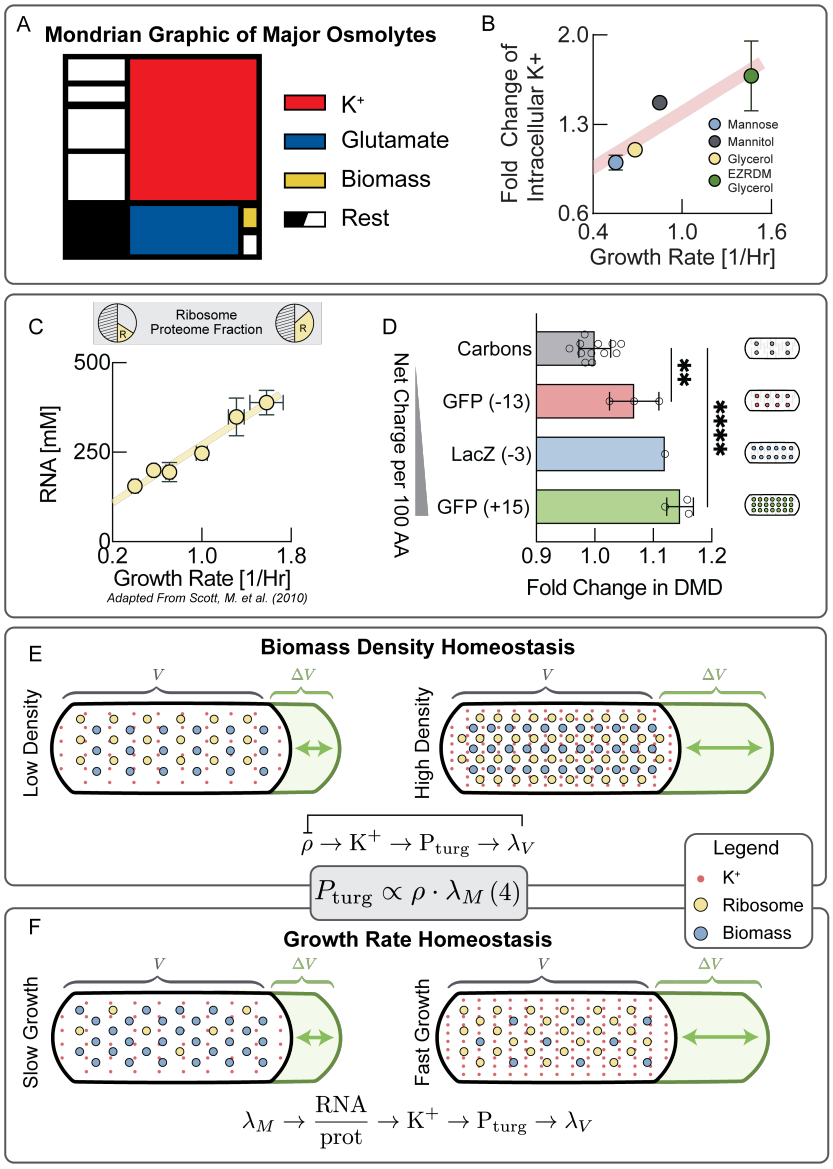

Figure 5: Ribosomal counterions act as the pacemaker of cell volume expansion. A, *Schematic illustration of major cellular osmolytes and their contribution to osmotic pressure.* ***B,*** *Intracellular*

potassium measured using mass spectrometry in low potassium medium in different growth condition. Each data point is determined from several measurements along the growth curve (see Fig. S10 for individual measurements, two biological replicates for each condition). Note that potassium diffuses out of the cell during the mandatory washing step with potassium free medium. This means that we cannot infer absolute intracellular concentrations and only relative changes of intracellular potassium across conditions. Error bars represent uncertainty of the fit in Fig. S10. ***C,*** *RNA/protein ratio changes with growth rate according to growth laws. We converted RNA/protein measurements, including error bars, from Scott et al. (*21*) to charge concentrations using total protein and total dry mass measurements from Basan et al. (*4*) (see Fig. S11), as well as dry mass density measurements from this work. Counterions balancing net charge of RNA are sufficient to account for the change in turgor pressure across growth rates.* ***D,*** *Biomass density increases continuously with overexpression of more positively charged proteins demonstrating the central role of charge balance for biomass density homeostasis. RNA carries one negative charge per nucleotide, whereas proteins are much less negatively charged. Therefore, there is an increase in biomass density in all conditions, but its magnitude depends on net protein charge. Because protein overexpression results in very long cells of irregular shape, biomass densities were determined using Threshold Iterative Volume (TIV) method (see Materials and Methods). Biological replicates shown as individual data points. Error bars are standard deviations from these biological replicates. P-values: **: 0.0042; ****: <0.0001.* ***E,*** *Turgor pressure generated by counterions of ribosomal RNA result in turgor pressure proportional to biomass density because ribosomes are a major component of biomass density (Eq. (4)). Together with the pacemaker model of cell volume expansion (Box 1), this results in homeostatic feedback control of cellular biomass density. Higher biomass density results in higher turgor pressure (Eq. (4)) and thereby faster cell volume expansion (Box 1, Eq. (3)).* ***F,*** *Due to bacterial growth laws (*21*), a larger fraction of biomass is made up of ribosomes in fast-growing cells as compared to slow-growing cells (higher RNA/protein ratio). This results in a higher molarity of counterions per biomass. At constant biomass density, faster growing cells thus have a higher counterion concentration and correspondingly a higher turgor pressure (Eq. (4)), as we observed experimentally (Fig. 1C). Higher turgor thus results in faster cell volume expansion, according to the pacemaker model of cell volume expansion (Box 1, Eq. (3)). This faster cell volume expansion is required for maintaining constant biomass density across growth rates (see Fig. 2A & Eq. (S5)).*

So far, our results indicate that an increase in turgor pressure with growth rate (Fig. 1) is indeed crucial for homeostasis of biomass density across growth rates (Fig. 2), enabled by endopeptidase-mediated cell wall fluidization (Fig. 3). But how is this increase in turgor pressure controlled and regulated? Osmotic pressures like turgor pressure are directly determined by molarities of osmolytes (Fig. 5A). Potassium is by far the most abundant cellular osmolyte in *E. coli* with estimated concentrations surpassing the combined concentrations of cellular other osmolytes (*6*) and therefore presumably the biggest contributor to turgor pressure. To test if the observed increase in turgor pressure originated from changes in potassium concentrations, we measured intracellular potassium on different substrates using mass spectrometry. Indeed, we found a striking linear increase in intracellular potassium with growth rate (Fig. 5B), similar to the increase in turgor pressure that we observed (Fig. 1C).

These data suggest that the observed increase in turgor pressure (Fig. 1) is likely due to an increase in intracellular potassium. But how does the cell regulate intracellular potassium and achieve this

increase in intracellular potassium concentration in precise coordination with growth rate? Potassium is positively charged, while the net charge of the cytoplasm must be neutral (*22*, *23*). Therefore, growth-rate dependent potassium concentrations must be balanced by an equivalent negative growth-rate dependent charge concentration in the cytoplasm. The concentration of the major intracellular anion glutamate has been shown to be roughly constant across growth rates (*24*) and thus cannot account for potassium charge balance across growth rates. However, an even bigger contribution to cytoplasmic charge comes from cellular RNA, as each nucleotide carries a negative elementary charge. Moreover, cellular RNA content as a fraction of biomass composition is well-known to increase with increasing growth rates, as measured by RNA to protein ratio (*21*). This is largely the result of an increase in ribosomal RNA with faster growth rates. When we converted the RNA to protein ratios across growth rates, measured by Scott et al. (*21*), to an intracellular charge concentration by using our own measurements of biomass density, combined with earlier measurements of total protein and total dry mass across growth conditions (*4*) (see Fig. S11), we indeed found that the resulting charge concentrations presented in Fig. 5C, were sufficient to account for the observed growth-rate dependent increase in turgor (Fig. 1C).

Based on these data, we propose that changes in turgor pressure across growth rates are mediated by changes in ribosomal RNA and the corresponding retention of potassium in the cytoplasm as RNA counterions, dictated by cellular charge balance. We previously proposed that biomass counterions may contribute to dry mass density homeostasis (*4*) and we realized that the contribution from ribosomal RNA, shown in Fig. 5B, far outweighs the contribution from other biomass components. To test this hypothesis experimentally, we investigated how changes in net cytoplasmic charge are reflected in cellular biomass density. If charge balance were indeed the key determinant of turgor driving envelope expansion, then overexpressing large quantities of proteins of different net charge should affect charge balance and be directly reflected in changes in cellular biomass density. More positively charged proteins should result a larger increase in biomass density. To test this prediction, we used an established system for expression of large quantities of useless proteins (*25*) to overexpress proteins of different net charge, including positively and negatively supercharged versions of GFP, developed by the Liu lab (*26*). Indeed, we found that biomass density continuously increased with the net positive charge per amino acid of the overexpressed protein (Fig. 5D), just as expected if turgor is controlled via charge balance.

By controlling turgor pressure via cellular charge, dominated by ribosomal RNA, bacteria elegantly achieve homeostatic feedback control of biomass density and coordination of cell wall expansion with growth rate: On the one hand, because turgor pressure is proportional to biomass density (Fig. 5, Eq. (4)), denser cells have higher turgor from a higher counterion concentration. According to the pacemaker model of cell volume expansion, this results in faster volume expansion (Box1, Eq. (3)), together constituting a negative homeostatic feedback loop, controlling biomass density (Fig. 5E).

On the other hand, bacterial growth laws mandate higher ribosomal RNA content with increasing growth rates for efficient self-replication (*21*). Thus, this automatically results in an increase in turgor pressure generated per biomass due to a larger fraction of ribosomal RNA (Fig. 5F & Eq. (4)). Higher turgor results in faster cell wall expansion according to the pacemaker model of cell volume expansion (Box1, Eq. (3)), which is precisely the requirement for maintaining constant biomass density across growth rates (Fig. 2 & Eq. (S5)). Thus, the cell achieves both homeostatic

feedback control on biomass density, as well as constancy of biomass density across a large range of growth rates, without the need for fine-tuned regulatory coordination between cell wall synthesis and biomass production rates.

The coupling between biomass and turgor pressure given by Eq. (4) can explain elegant experiments that led to the observation that after short osmotic shocks that put cells into plasmolysis, cell length quickly relaxes back to the length that cells would have attained had they never been plasmolyzed (*2*). Because biomass growth proceeds during plasmolysis, the feedback loop given in Fig. 5D will restore biomass density and therefore cell volume to where it would have been without an osmotic shock. The detailed temporal dynamics of this relaxation depend on cell wall rheology. In a viscoelastic Maxwell rheology (Eq. (1)), a very fast initial elastic relaxation would be followed by a slower viscous relaxation phase. More experimental work, including systematic osmotic shifts of different magnitudes and durations are needed to detect these subtle differences in relaxation dynamics and calibrate parameters of cell wall rheology.

Biomass production and cell wall synthesis are two seemingly disjoint cellular processes that must nevertheless be tightly physiologically coordinated to ensure survival and efficient growth. Without coordination of biomass production and cell envelope expansion, cells would encounter molecular crowding disrupting metabolic processes and growth or lyse, either from a buildup of turgor or from excessive cell wall expansion, exceeding biosynthetic capacity. Moreover, a substantial fraction of cellular resources is devoted to synthesis of the bacterial cell wall (*27*). Thus, for optimal growth, synthesis of cell wall precursors and the cell wall itself must be coordinated with biomass synthesis. It has long been unclear how bacteria achieve this remarkable feat. Our work shows that cell wall expansion is in fact intimately coupled with biomass synthesis. Ribosome-determined turgor pressure acts as the pacemaker of volumetric growth.

Interestingly, the pacemaker role of turgor pressure is consistent with our recent findings that starving bacteria expend the lion's share of their ATP maintenance budget to maintain plasmolysis by exporting ions to reduce turgor (*28*). Plasmolysis is a state with vanishing turgor pressure. According to the pacemaker model of cell volume expansion (Box1, Eq. (3)), vanishing turgor is required to stop the expansion of the cell envelope in starving bacteria. Hence, a buildup of turgor would result in uncontrolled cell volume expansion. In the absence of cell wall precursor synthesis to reinforce the cell wall in starvation conditions, this would result in lysis and cell death. Indeed, this is precisely what we observe in starving bacteria after loss of ion homeostasis due to lack of ATP prior to cell death (*28*).

In conclusion, we believe that these simple, yet elegant mechanisms of coordination play a central role in cell physiology. While we focused on the model organism *E. coli* in this work, these mechanisms are likely conserved across evolution, extending to other microbial species. Mechanical pressure generated by fast-growing, ribosome-rich cancer cells may even enable their aggressive expansion in a competition for space inside healthy tissues (*29–32*).

Acknowledgements
We would like to thank Terry Hwa for lively discussions about these topics and much helpful advice and suggestions. We would also like to thank Becky Ward, Quincey Justman, Ariel Amir, Joshua Rabinowitz and Jan Skotheim for helpful feedback on the manuscript. We would also like

to thank Jennifer Waters and Talley Lambert (Nikon Imaging center, Harvard medical school), for valuable comments on image acquisition and processing. We thank Charles Langmuir for giving us access to ICP-MS facility and thanks to Zhongxing Chen for helping us with the ICP-MS experiments. We thank Michael Springer of Harvard medical school for giving us access to CellAsic microfluidics device and special thanks to Ang Li (Springer lab) for technical troubleshooting with this device. This project was supported by MIRA grant (5R35GM137895) and an HMS Junior Faculty Armenise grant to MB.

References

1. E. R. Rojas, K. C. Huang, Regulation of microbial growth by turgor pressure. *Curr Opin Microbiol*. **42**, 62–70 (2018).
2. E. Rojas, J. A. Theriot, K. C. Huang, Response of Escherichia coli growth rate to osmotic shock. *Proceedings of the National Academy of Sciences*. **111**, 7807–7812 (2014).
3. F. Wong, L. D. Renner, G. Özbaykal, J. Paulose, D. B. Weibel, S. van Teeffelen, A. Amir, Mechanical strain sensing implicated in cell shape recovery in Escherichia coli. *Nat Microbiol*. **2**, 17115 (2017).
4. M. Basan, M. Zhu, X. Dai, M. Warren, D. Sévin, Y.-P. Wang, T. Hwa, Inflating bacterial cells by increased protein synthesis. *Mol Syst Biol*. **11**, 836 (2015).
5. E. R. Oldewurtel, Y. Kitahara, S. van Teeffelen, Robust surface-to-mass coupling and turgor-dependent cell width determine bacterial dry-mass density. *Proceedings of the National Academy of Sciences*. **118** (2021), doi:10.1073/PNAS.2021416118.
6. D. S. Cayley, H. J. Guttman, M. T. Record, "Biophysical Characterization of Changes in Amounts and Activity of Escherichia coli Cell and Compartment Water and Turgor Pressure in Response to Osmotic Stress" (2000).
7. L. Gerosa, B. R. B. Haverkorn van Rijsewijk, D. Christodoulou, K. Kochanowski, T. S. B. Schmidt, E. Noor, U. Sauer, Pseudo-transition Analysis Identifies the Key Regulators of Dynamic Metabolic Adaptations from Steady-State Data. *Cell Syst*. **1**, 270–282 (2015).
8. C. You, H. Okano, S. Hui, Z. Zhang, M. Kim, C. W. Gunderson, Y.-P. Wang, P. Lenz, D. Yan, T. Hwa, Coordination of bacterial proteome with metabolism by cyclic AMP signalling. *Nature*. **500**, 301–6 (2013).
9. S. Hui, J. M. Silverman, S. S. Chen, D. W. Erickson, M. Basan, J. Wang, T. Hwa, J. R. Williamson, Quantitative proteomic analysis reveals a simple strategy of global resource allocation in bacteria. *Mol Syst Biol*. **11** (2015), doi:10.15252/msb.20145697.
10. L. K. Harris, J. A. Theriot, Relative rates of surface and volume synthesis set bacterial cell size. *Cell*. **165**, 1479–1492 (2016).
11. K. C. Huang, R. Mukhopadhyay, B. Wen, Z. Gitai, N. S. Wingreen, Cell shape and cell-wall organization in Gram-negative bacteria. *Proc Natl Acad Sci U S A*. **105**, 19282–19287 (2008).
12. A. Amir, F. Babaeipour, D. McIntosh, D. Nelson, S. Jun, Bending forces plastically deform growing bacterial cell walls. *Proc Natl Acad Sci U S A*. **111** (2014).
13. J. Ranft, M. Basan, J. Elgeti, J.-F. Joanny, J. Prost, F. Jülicher, Fluidization of tissues by cell division and apoptosis. *Proc Natl Acad Sci U S A*. **107**, 20863–20868 (2010).
14. A. Amir, D. R. Nelson, Dislocation-mediated growth of bacterial cell walls. *Proc Natl Acad Sci U S A*. **109**, 9833–9838 (2012).

15. K. Kruse, J. F. Joanny, F. Jülicher, J. Prost, K. Sekimoto, Generic theory of active polar gels: a paradigm for cytoskeletal dynamics. *The European Physical Journal E*. **16**, 5–16 (2005).
16. S. K. Singh, L. SaiSree, R. N. Amrutha, M. Reddy, Three redundant murein endopeptidases catalyse an essential cleavage step in peptidoglycan synthesis of *Escherichia coli* K12. *Mol Microbiol*. **86**, 1036–1051 (2012).
17. S. Klumpp, Z. Zhang, T. Hwa, Growth rate-dependent global effects on gene expression in bacteria. *Cell*. **139**, 1366–75 (2009).
18. G. Kapoor, S. Saigal, A. Elongavan, Action and resistance mechanisms of antibiotics: A guide for clinicians. *J Anaesthesiol Clin Pharmacol*. **33** (2017), pp. 300–305.
19. S. Hussain, C. N. Wivagg, P. Szwedziak, F. Wong, K. Schaefer, T. Izoré, L. D. Renner, M. J. Holmes, Y. Sun, A. W. Bisson-Filho, S. Walker, A. Amir, J. Löwe, E. C. Garner, MreB filaments align along greatest principal membrane curvature to orient cell wall synthesis. *Elife*. **7** (2018), doi:10.7554/eLife.32471.
20. S. Van Teeffelen, S. Wang, L. Furchtgott, K. C. Huang, N. S. Wingreen, J. W. Shaevitz, Z. Gitai, The bacterial actin MreB rotates, and rotation depends on cell-wall assembly. *Proc Natl Acad Sci U S A*. **108**, 15822–15827 (2011).
21. M. Scott, C. W. Gunderson, E. M. Mateescu, Z. Zhang, T. Hwa, Interdependence of cell growth and gene expression: origins and consequences. *Science*. **330**, 1099–102 (2010).
22. B. Hille, "Ion channels of excitable membranes" in (2001).
23. T. P. Ikeda, A. E. Shauger, S. Kustu, Salmonella typhimuriumApparently Perceives External Nitrogen Limitation as Internal Glutamine Limitation. *J Mol Biol*. **259**, 589–607 (1996).
24. K. Kochanowski, H. Okano, V. Patsalo, J. Williamson, U. Sauer, T. Hwa, Global coordination of metabolic pathways in Escherichia coli by active and passive regulation. *Mol Syst Biol*. **17**, e10064 (2021).
25. M. Basan, S. Hui, H. Okano, Z. Zhang, Y. Shen, J. R. Williamson, T. Hwa, Overflow metabolism in Escherichia coli results from efficient proteome allocation. *Nature*. **528** (2015), doi:10.1038/nature15765.
26. D. B. Thompson, J. J. Cronican, D. R. Liu, Engineering and identifying supercharged proteins for macromolecule delivery into mammalian cells. *Methods Enzymol*. **503**, 293–319 (2012).
27. F. C. Neidhardt, 1931-, J. L. Ingraham, Moselio. Schaechter, Physiology of the bacterial cell (1990) (available at http://agris.fao.org/agris-search/search.do?recordID=US201300651900).
28. S. Schink, M. Polk, E. Athaide, A. Mukherjee, C. Ammar, X. Liu, S. Oh, Y.-F. Chang, M. Basan, *bioRxiv*, in press, doi:10.1101/2021.11.22.469587.
29. M. Basan, T. Risler, J.-F. Joanny, X. Sastre-Garau, J. Prost, Homeostatic competition drives tumor growth and metastasis nucleation. *HFSP J*. **3**, 265–272 (2009).
30. R. Levayer, Solid stress, competition for space and cancer: The opposing roles of mechanical cell competition in tumour initiation and growth. *Semin Cancer Biol* (2019), , doi:10.1016/j.semcancer.2019.05.004.
31. E. Moreno, L. Valon, F. Levillayer, R. Levayer, Competition for Space Induces Cell Elimination through Compaction-Driven ERK Downregulation. *Current Biology*. **29**, 23-34.e8 (2019).

32. R. Levayer, C. Dupont, E. Moreno, Tissue Crowding Induces Caspase-Dependent Competition for Space. *Curr Biol*. **26**, 670–7 (2016).